Georadar for hydrogeology[1]

R.A. van Overmeeren[2]

Introduction

Falling water tables and deteriorating water quality are the major shallow hydrogeological problems currently facing groundwater management in the Netherlands; the former phenomenon is seriously affecting agriculture and nature conservation, whereas shallow contaminated groundwater is a hazard for water supply companies and is also an environmental threat. Predictive scenarios are used when planning appropriate management strategies to deal with these problems. These scenarios use models of groundwater flow. Detailed imaging and accurate characterization of the shallow subsurface (down to about 50 m) are essential for the reliability of these models and consequently for the success of groundwater management.

Since the 1950s, various non-destructive geophysical methods have been important in groundwater exploration in the Netherlands, but they have shortcomings. lectrical and electromagnetic methods tend to have sufficient resolution for very shallow and detailed mapping, whereas high-resolution seismic reflection is currently not effective at depths less than about 30 m. Moreover, in many cases seismic reflection is too expensive for groundwater applications.

Ground penetrating radar (GPR) is a geophysical technique related to seismic reflection; both methods are based on wave propagation and provide very detailed and continuous images of the subsurface. The two methods are complementary: the deep subsurface is the domain of seismic reflection and is beyond the reach of GPR, but in the shallow zones radar offers an attractive and cost-effective alternative. GPR has been used successfully in geotechnical investigations for over a decade (Ulriksen 1982; Hänninen 1992; Saarenketa *et al.* 1992), generally to depths of a few metres. Recent developments in digital instrumentation and low-frequency antennas (Davis and Annan 1989) have extended the GPR domain in radar-favourable areas (low soil conductivities) to depths of several tens of metres, making the method suitable for geological applications; hence the name 'georadar'. Jol and Smith (1992) describe geological applications of georadar in Canada, and Beres and Haeni (1991) give hydrogeological examples from the USA.

Water supply companies in the east of the Netherlands are finding it difficult to model groundwater flow in areas of push moraines, where groundwater levels change abruptly (in 'steps'), presumably because of thin, steeply dipping, poorly permeable clay layers between the sand layers of the aquifers (Fig. 2a). The evidence for the existence of these clay layers is found in geophysical well logs from water wells in the area and in the measured fluctuations of the water table. Attempts to map these layers using DC resistivity, seismic refraction, FEM and TEM, and high-resolution seismic reflection have failed. Eight water companies, therefore, decided to pool their efforts and set up a foundation that aims to optimize GPR techniques for applications to hydrogeological and related environmental and ecological investigations in groundwater supply areas.

An extensive programme of field measurements was conducted in more than twenty pilot areas, on targets representing the major hydrogeological features in the shallow subsurface of interest to the water supply companies. The measurements were made with a PulseEKKO IV radar system (Davis and Annan 1989), with antennas of 200, 100, 50 and 25 MHz.

This paper presents characteristic examples of measured sections to illustrate the potential of the georadar technique for hydrogeological applications.

Hydrogeology and physical properties

Reflection of radar waves

The success of geophysical exploration methods depends on contrasts in physical properties in the subsurface. The physical property that determines the reflection of electromagnetic waves is the dielectric constant or permittivity ε (Olhoeft 1987; Davis and Annan 1989); the propagation velocity of radar waves also depends directly on this property. Fortunately, important hydrogeological boundaries generate substantial permittivity contrasts (Table 1). The large contrast in ε between dry and water-saturated sands make the water table a splendid reflector of radar waves, a feature which is enhanced by its smooth surface. Peat, whose dielectric constant approaches that of water, also contrasts distinctly with other deposits, and is therefore well reflected in radargrams (Ulriksen 1982). The dielectric constant of clays varies over a broad range; hence in radar sections clays may be visible at some locations but remain undetected in others.

---

sented at the 55th Meeting of the EAEG, Stavanger June 1993.

NO Institute of Applied Geoscience, PO Box 6012, 2600 JA Delft, The Netherlands.

Table 1. Characteristic values of physical properties of media important for georadar (after Davis and Annan 1989; Hänninen 1992).

Medium	Dielectric constant ε	Propagation velocity v (cm ns^{-1})	Attenuation α (dB m^{-1})
Air	1	30	0
Dry sand	4	15	0.01
Water saturated sand	25	6	0.03–0.3
Clays	5–40	4.7–13	1–300
Peat	60–80	3.9–3.4	0.3
Water (fresh)	80	3.4	0.1
Water (saline)	80	3.4	1000

Attenuation and resolution of radar waves

Another electrical property, the electrical resistivity ρ, determines the attenuation of radar waves and thus the exploration depth that can be reached. The lower the resistivity, the smaller the radar penetration depth. In practice, georadar is unfit for use in areas where the soil resistivity is less than 100 Ωm; this is the case in clayey and silty formations and in brackish and saline groundwater environments. As a consequence, georadar cannot be applied in most of the western part of the Netherlands. The degree of attenuation is expressed by the attenuation factor α (in dB m^{-1}); characteristic values are given in Table 1.

The exploration depth also depends on the frequency of the radar pulse; the lower the frequency, the greater the penetration capacity. Such an increase of exploration depth through frequency, however, is achieved at the expense of resolution. This is illustrated in Fig. 1, in which radar sections recorded along a 50-m profile are compared using four of the available frequencies of the PulseEKKO system: 25, 50, 100 and 200 MHz. Continuous reflectors with a relatively large amplitude, often typical of the water table, are observed in the 25 MHz section at 160 and 430 ns, corresponding to inferred depths (at a constant propagation velocity of 13.5 cm ns^{-1}) of about 11 and 29 m respectively. Data from a well at this location indicate that the shallow reflector correlates with a perched water table, maintained by a thin (5 cm) loam layer. The deep reflector agrees with the true, regional water table. Because of the low frequency, the wavelength is large and individual layers can barely be distinguished, if at all; i.e. the resolution is poor.

More detail is observed in the 50 MHz section. The exploration depth, however, has decreased and the deep water table is no longer visible as a continuous reflector. The exploration depth decreases even more in the 100 and 200 MHz sections. The resolution in these sections has improved; the perched water table has become a

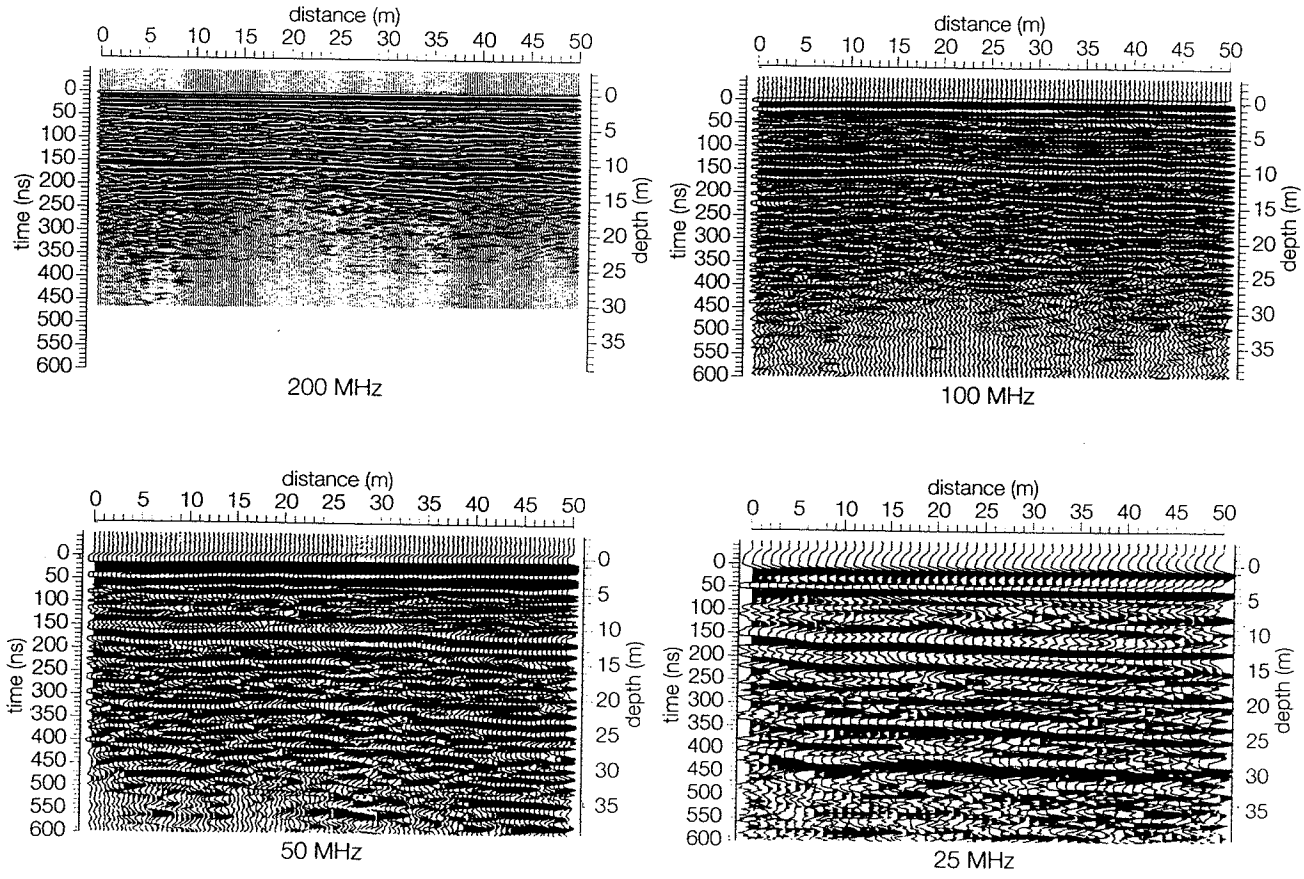

Fig. 1. Georadar sections illustrating the influence of radar frequency on exploration depth and resolution (propagation velocity is 13.5 cm ns^{-1})

narrow band whose depth can be read with great precision. More and more detail is also observed in the dry zone above the perched water table.

Hydrogeological applications of georadar in the Netherlands

During the project georadar measurements were made in more than twenty pilot areas in the Netherlands, selected for their relevance to hydrogeology and their suitability for georadar. The boundary conditions were the exploration depth (maximum 40 m) and the electrical resistivity of the subsurface (more than 100 Ωm). An important criterion for the site selection was the availability of additional information from boreholes and observation wells for the verification of the radar surveys.

The hydrogeological targets of georadar in the Netherlands can be grouped into four categories (Fig. 2):

- Mapping tectonic and sedimentary structures.
- Mapping water tables in sandy deposits of push moraines, river terraces and sand dunes.
- Mapping perched water tables and distinguishing these from true water tables.
- Determining the lateral extent and continuity of clay and peat layers.

Deep water tables and geological structures in push moraines

As implied earlier, the precise imaging of the deep water tables found in the higher-lying parts of the Netherlands is important for modelling groundwater flow. Georadar can provide valuable model parameters such as the steps in groundwater levels created by poorly permeable layers and layer structures (Fig. 2a and b). These phenomena are particularly important in ice-pushed ridges, which consist mainly of sandy unconsolidated river deposits deformed by glaciotectonic action during Pleistocene glacials.

A typical example featuring both a deep regional water table and geological structure is shown in the radar section of Fig. 3. The profile was measured with 50 MHz antennas and a station interval of 0.5 m; the section has been corrected for topography and has identical horizontal and vertical scales. The deepest reflector is the water table, which is approximately 40 m below the surface. The sedimentary structures illustrate the transition from the flat glacial outwash in the west to the dipping structures of a push moraine in the east (cf. target sketch, Fig. 2a); an anticline is clearly visible in the smoothly curved, continuous reflector of high amplitude.

Another example (Fig. 4) of deep water tables and geological structures ilustrates the potential and limitations of georadar. This profile was recorded with 25 MHz antennas and a station interval of 1 m; the section has been corrected for topography and has identical horizontal and vertical scales. The water table is recognizable as a horizontal reflector of large amplitude. In the northern part of the profile the reflector is continuous; in the southern, most elevated part, it is only visible fragmentarily. Evidently, the limits of the exploration depth are reached here. Conversion from time to depth is based on a wave propagation velocity of 14.5 cm ns^{-1} determined from common midpoint (CMP) measurements. The greatest depth at which the water table is still visible is 42 m. Deep water tables commonly constitute the deepest visible reflector, because much energy is reflected at this interface as a result of the great

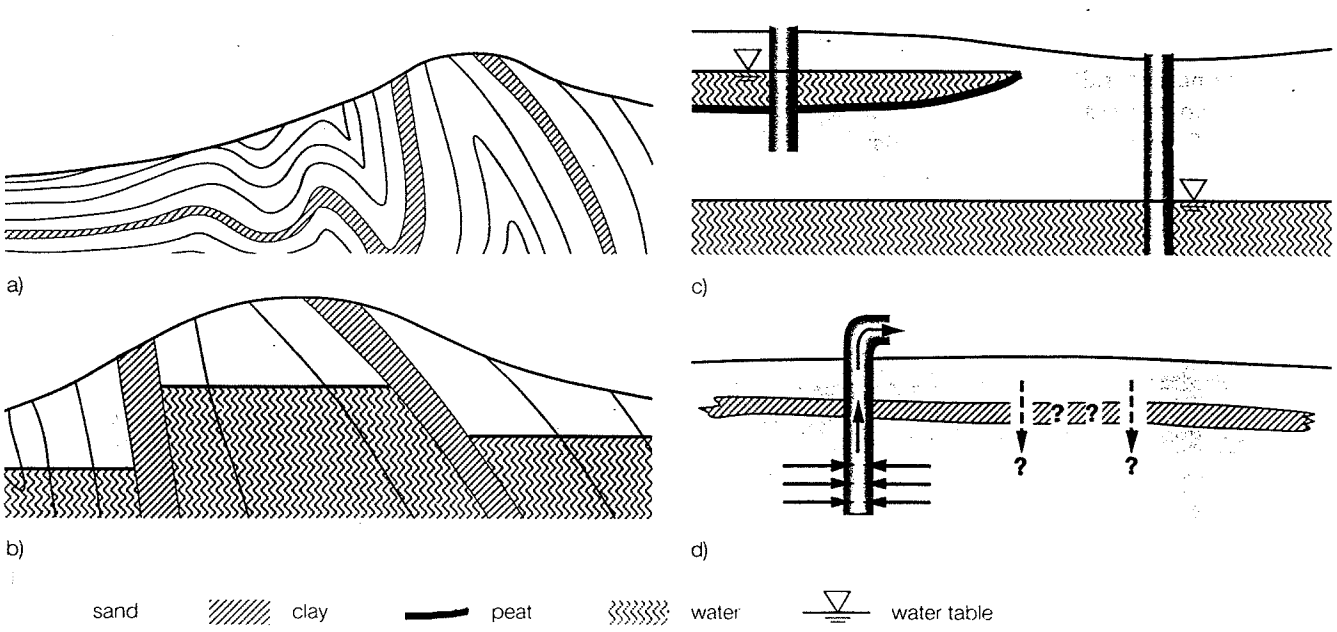

Fig. 2. Hydrogeological targets of georadar: (a) geological structures; (b) Steps in water table; (c) perched water table; (d) extent and continuity of semi-pervious clay and peat layers.

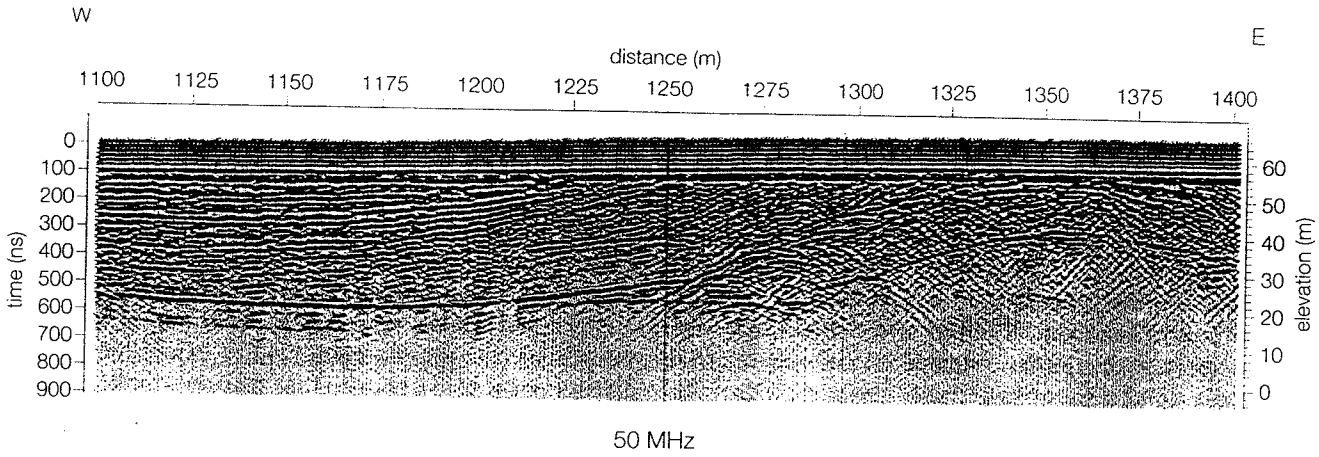

Fig. 3. A georadar section (50 MHz) showing the transition from glacial outwash (west) to push moraine sediments (east); in the western part a deep water table is reflected.

contrast between the dielectric constants of dry and water-saturated sands (Table 1). Geological structures are visible above the water table; oblique reflectors represent inclined layers. These reflectors are interfaces between sandy layers of different grain size or between sandy and clayey sediments; both transitions give rise to contrasts in moisture content, i.e. contrasts in dielectric constants. A conspicuous reflector of large amplitude and dipping to the south is visible in the centre of the section. A small offset in depth can be seen between the water tables on either side of this reflector. Even though this offset of approximately 2 m is only slightly more than the resolution of the 25 MHz antennas, it seems likely that there is a step in the water table here, caused by a clay layer which produces the prominent image of a dipping reflector (cf. target sketch, Fig. 2b).

Steps in the water table

Sandy ice-pushed ridges also contain shallower water tables, as shown by the profiles in Fig. 5 measured near a well field of a regional water supply company. Because of the shallower depths, 100 MHz antennas could be used; the station interval was 0.5 m. Both sections of 190 m length are parts of longer profiles that run parallel, 250 m apart. The sections have been corrected for topography; the vertical scales are twice the horizontal scales. The water table, between 5 m and 10 m below the surface, is clearly visible as a continuous, horizontal reflector of large amplitude. Both sections are magnificent examples of sudden and pronounced steps in groundwater levels (compare target sketch, Fig. 2b). In profile 2, diffraction tails are visible on both sides of the offset. Loss of energy at the groundwater step might indicate attenuation due to a dipping clay layer. In contrast, the offset observed in profile 3 is amazingly razor-sharp. No evidence of separating impermeable layers is visible in the radar image. To exclude the possibility that the observed offset is caused by a sudden change in wave propagation velocity rather than by a groundwater step, CMP measurements were performed on both sides of the feature (Fig. 6). Velocity analysis of the CMP data shows that the small velocity contrast calculated (13 vs. 14 cm ns^{-1}) does not account for the observed offset in the reflector, but even enhances the effect.

The offset is about 2.5 m. Additional parallel radar profiles allowed the groundwater step to be traced a further 750 m southwards. All pumping wells are located east of the boundary, where the water table is

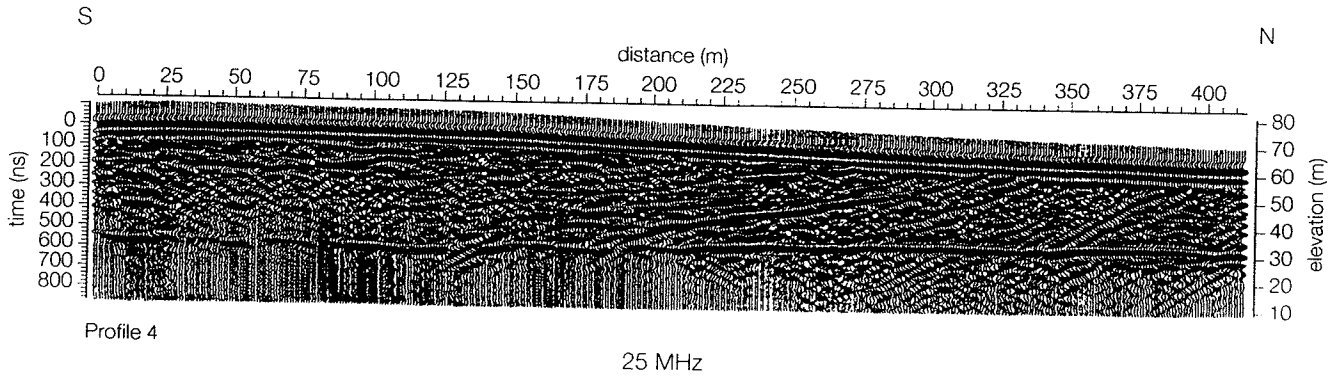

Fig. 4. A georadar section (25 MHz) showing a deep water table in dipping, mainly sandy deposits of a push moraine.

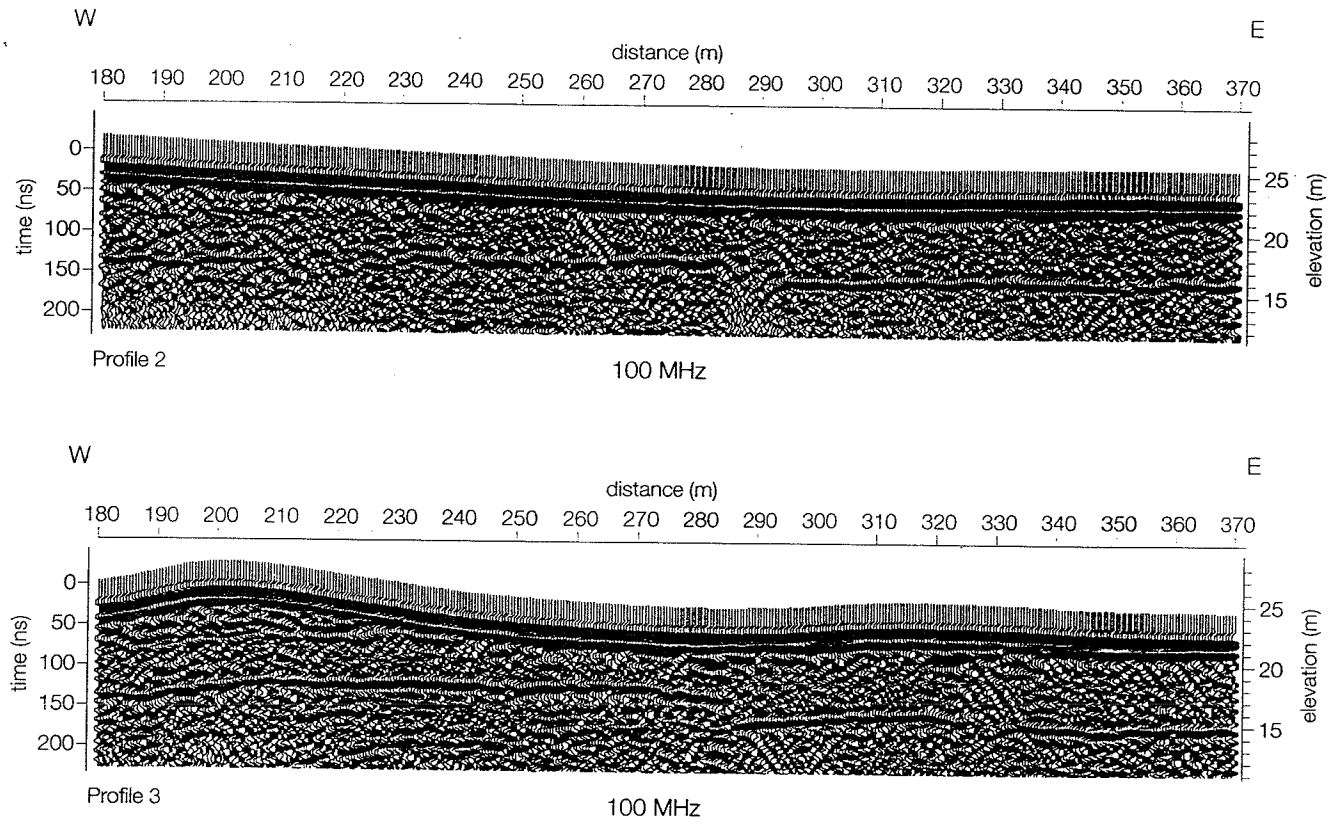

Fig. 5. Georadar sections (100 MHz) showing steps in water table in push moraine deposits, observed along parallel profiles 250 m apart.

lower. Obviously, west of the boundary the influence of the well field is greatly reduced by the sealing effect of the separating dipping layer.

Peat and perched water tables

Perched water tables, if not recognized as such, may yield erroneous gradients in groundwater levels

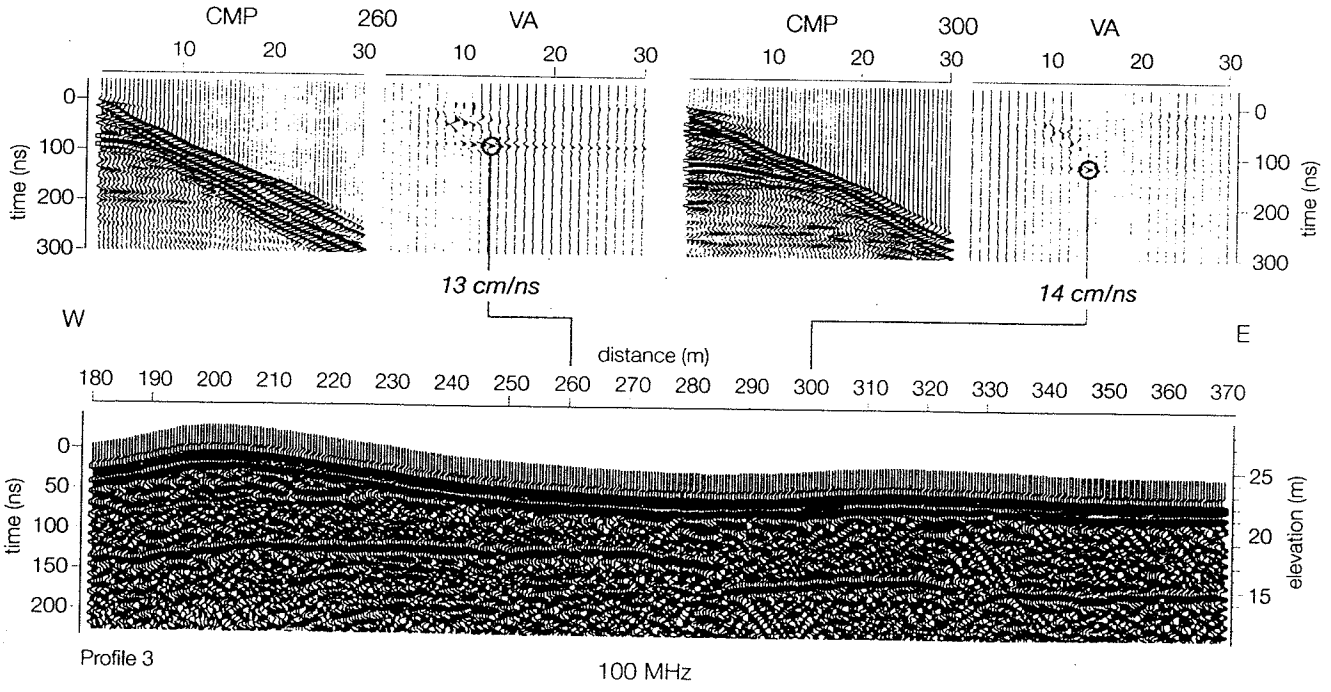

Fig. 6. Velocity analysis (VA) of CMP measurements made on either side of the groundwater step observed in push moraine deposits (profile 3 of Fig. 5).

(cf. target sketch, Fig. 2c). Perched groundwater in the coastal sand dunes of the Amsterdam water supply company is sustained by shallow peat layers that are only about 5–20 cm thick. Areas where peat layers maintain shallow groundwater have moist soils and are relatively insensitive to the effects of groundwater abstraction from the regional aquifer. The peat occurrences are thus of great importance both for groundwater flow modelling and for ecological equilibrium.

Prior to the georadar survey, the Dutch Geological Survey investigated the extent of peat layers in parts of the study areas by drilling a large number of boreholes with depths ranging from 5 to 11 m. But boreholes disturb the thin sealing peat layers and, moreover, merely provide point information. Georadar not only produces continuous images of the peat layers, but also of the water tables—whether perched or regional. All these interfaces are clearly visible in radar images because of the large contrast in dielectric constants between dry sands, water-saturated sands and peat (Table 1). The high value of the dielectric constant makes peat detectable, even below the water tables.

The georadar section of Fig. 7a, recorded with 100 MHz antennas and a station interval of 0.5 m, illustrates the above. The high frequency provides much detail and could be applied because of the shallow depths of the targets. The vertical scale is six times the horizontal one, producing strong exaggeration of structures. The radargram was interpreted (Fig. 7b) using additional information from observation wells and boreholes made to verify the georadar measurements (Fig. 7c). The weirdly shaped reflector correlates with the peat layer, which has its eastern boundary near radar station 35. The peat layer sustains perched groundwater found at a depth of about 2.5 m; the perched water table is a flat reflector which slopes gradually eastwards with the topography and is bounded by the edge of the peat near station 35. East of this point the water table is found at a depth of 5 m, as is measured in observation well 10j–151 (Fig. 7c). This is the regional water table, which is imaged in the radar section by the deepest continuous reflector. A CMP measurement at this location showed an average propagation velocity down to this reflector of 12 cm ns^{-1}, which corresponds to the velocity of radar waves in dry sands (Table 1). Reflections from the regional water table can be traced westwards until about station 180, no longer as a smooth line, but more or less following the shape of the overlying peat layer. This correspondence is attributable to lateral variations in velocity caused by differences in thickness of the perched aquifer, where the wave velocity is less than in the overlying and underlying dry layers. Owing to the vertical variations in velocity, the depth scale, which is valid for one velocity only, is not correct in the radar section. It is based on an average velocity and is only intended to give a general indication.

Mapping clay layers

The georadar section of Fig. 8a was recorded with 50 MHz antennas and a station interval of 0.5 m along a profile crossing a valley with marine interglacial deposits and continuing into an uplifted ridge of ice-pushed sediments (Fig. 8b). A clay layer forms part of the marine formation. The georadar survey aimed to map the clay layer and to establish its western limit (cf. target sketch, Fig. 2d). This clay layer, in the centre of the valley at a depth of 15 m, sustains an artesian aquifer which is recharged by infiltration in the higher ice-pushed ridge. It is important to map the clay boundaries precisely, for groundwater flow modelling.

The georadar section of Fig. 8a shows 375 m of the profile which is 3 km long. The vertical scale of the image is exaggerated compared to the horizontal by a factor of 2.5. The regional groundwater level is at a depth of approximately 7 m, as measured in an observation well slightly west of the radar section.

Velocity analysis of a CMP made near the well gave a velocity of 11.5 cm ns^{-1} for the sediments above the water table. In Fig. 8a the water table is depicted by the reflector at 100 ns. The clay reflector is identified by correlations with borehole 32D-93 (Fig. 8b), further east along the radar profile. In the radar section displayed (the depth scale is based on a propagation velocity of 9 cm ns^{-1}, the mean of the subsurface above and below the water table), this reflector is at a depth of 6 m below sea-level (15 m below the surface) in the east, near radar stations 2425. Westwards the depth decreases and the reflector peters out near radar station 2715, indicating the edge of the clay layer. Also very noticeable is the transition from a sub-horizontal stratification east of this edge, and the incoherent radar image with many disturbing diffraction hyperbolas to the west, which is characteristic of ice-pushed formations.

CMP measurements along the profile yielded velocities of 7.5 cm ns^{-1} for the formation above the clay reflector; this is irrefutable evidence of water-saturated sediments (Table 1). This example of a radar image of a clay layer below the water table is unusual. At many other locations in the Netherlands it proved impossible to detect clay layers below the water table. The successful result here is attributable to the high electrical resistivity of the subsurface and consequently the small attenuation of the radar waves in this area.

Conclusion

The extensive field measurements performed in selected pilot areas of the Netherlands demonstrate that georadar is a valuable and promising geophysical method for cost-effective imaging of the shallow subsurface down to a depth of 40 m. The radargrams obtained present extremely detailed continuous sections with a resolution that meets the requirements for groundwater flow modelling and ecological investigations of the shallow zones. The non-destructive georadar technique is particularly interesting for applications in sensitive environments, where drilling is undesirable.

Acknowledgements

I am grateful to the following water supply companies for their financial support and for their active and inspiring participation in the realization of the project: Veluwse Nutsbedrijven NV, NV Waterleiding Maatschappij Gelderland, NV Waterleidingmaatschappij

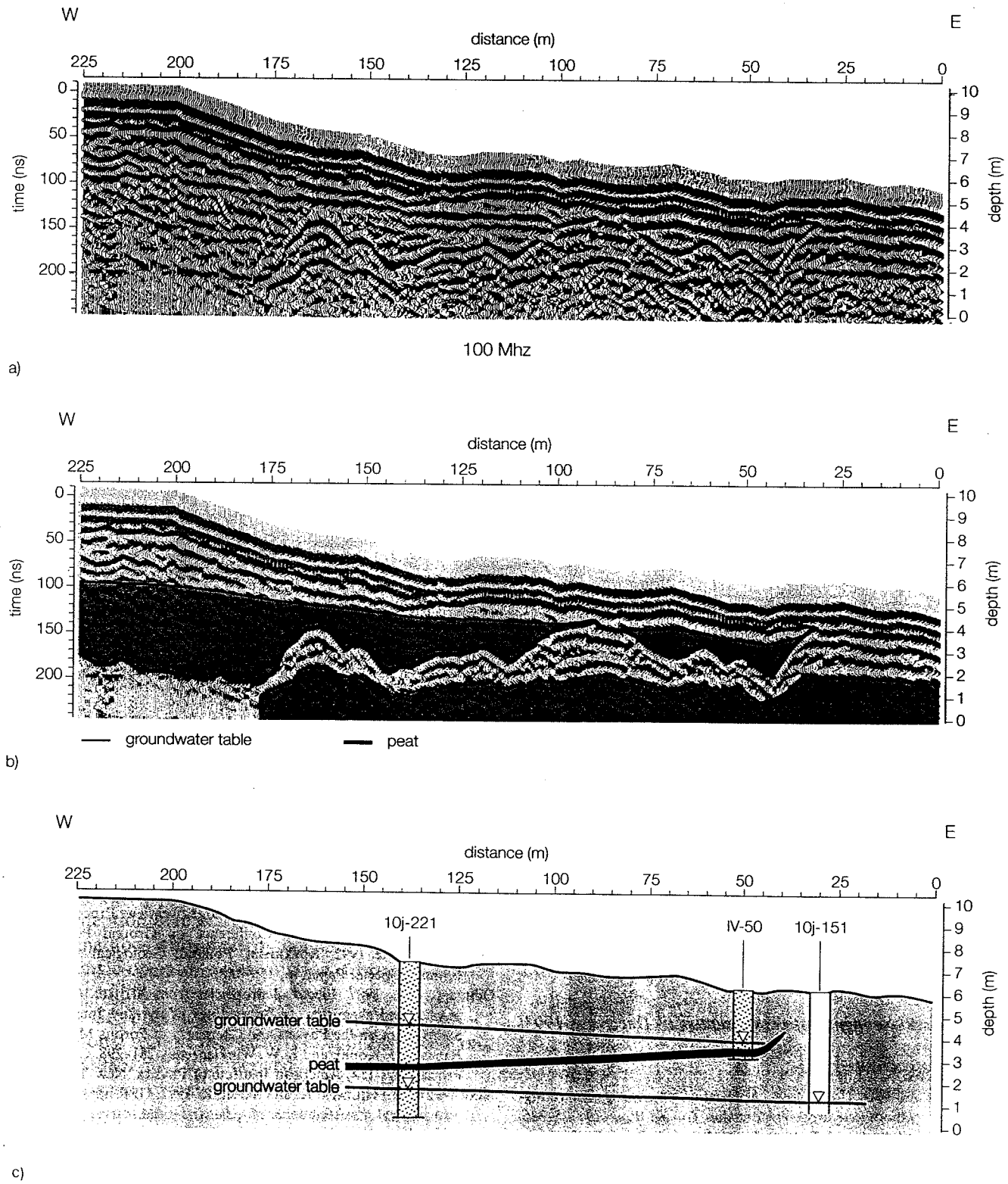

Fig. 7. Georadar section (100 MHz) in coastal sand dunes, showing a regional water table and a peat layer that sustains a perched water table: (a) radargram; (b) interpretation; (c) drilling evidence.

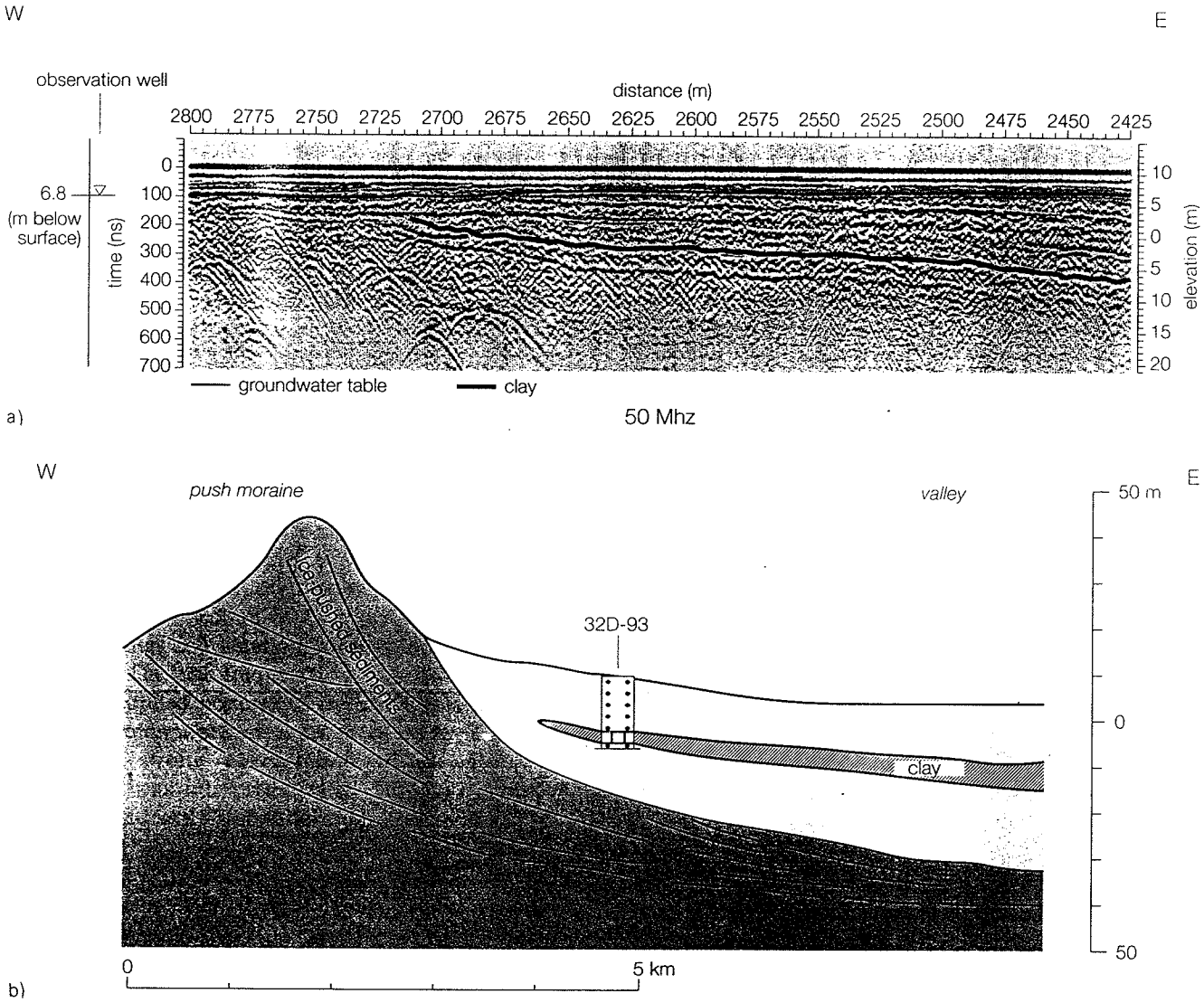

Fig. 8. (a) georadar section (50 MHz) with the edge of a clay layer below the water table. (b) Hydrogeological sketch of the clay target. The clay layer peters out near the valley border and the margin of an ice-pushed ridge.

Oostelijk Gelderland, PGEM, Waterleiding Maatschappij Overijssel NV, NV Waterleidingbedrijf Midden-Nederland, NV Waterleiding Maatschappij Limburg, Gemeente Waterleidingen Amsterdam. The project was subsidized by the Dutch Ministry of Economic Affairs. The illustrations were prepared by J. Rietstap (TNO).

Received 30 September 1993; accepted 17 December 1993.

References

BERES, M. and HAENI, F.P. 1991. Application of ground-penetrating-radar methods in hydrogeologic studies. *Ground Water* **29**, 375–386.

DAVIS J.L. and ANNAN, A.P. 1989. Ground-penetrating radar for high-resolution mapping of soil and rock stratigraphy. *Geophysical Prospecting* **37**, 531–551.

HÄNNINEN, P. 1992. Application of ground penetrating radar techniques to peatland investigations. Proceedings of the Fourth International Conference on Ground Penetrating Radar, June 1992, Rovaniemi, Finland: Geological Survey of Finland, Special Paper 16, 217–221.

JOL, H.M. and SMITH, D.G. 1992. Geometry and structure of deltas in large lakes: a ground penetrating radar overview. Proceedings of the Fourth International Conference on Ground Penetrating Radar, June 1992, Rovaniemi, Finland; Geological Survey of Finland, Special Paper 16, 159–168.

OLHOEFT, G.R. 1987. Electrical properties from 10^{-3} to 10^{+9} Hz—physics and chemistry. *In* Proceedings of the 2nd International Symposium on the Physics and Chemistry of Porous Media, J.R. Banavar, J. Koplik and K.W. Winkler (eds), 281–298. Conference Proceedings 154, American Institute of Physics, New York.

SAARENKETA, T., HIETALA, K. and SALMI, R. 1992. GPR applications in geotechnical investigations of peat for road survey purposes. Proceedings Fourth International Conference on Ground Penetrating Radar, June 1992, Rovaniemi, Finland; Geological Survey of Finland, Special Paper 16, 293–305.

ULRIKSEN, P. 1982. Application of impulse radar to civil engineering. Ph.D. thesis, Lund University of Technology, Sweden, Published by Geophysical Survey Systems Inc, Hudson, New Hampshire, USA.